Recruitment of an inhibitory hippocampal network after bursting in a single granule cell

Masahiro Mori*, Beat H. Gähwiler, and Urs Gerber

Brain Research Institute, University of Zurich, Winterthurerstrasse 190, CH-8057 Zurich, Switzerland

Communicated by Harald Reuter, University of Bern, Bern, Switzerland, March 12, 2007 (received for review January 5, 2007)

The hippocampal CA3 area, an associational network implicated in memory function, receives monosynaptic excitatory as well as disynaptic inhibitory input through the mossy-fiber axons of the dentate granule cells. Synapses made by mossy fibers exhibit low release probability, resulting in high failure rates at resting discharge frequencies of 0.1 Hz. In recordings from functionally connected pairs of neurons, burst firing of a granule cell increased the probability of glutamate release onto both CA3 pyramidal cells and inhibitory interneurons, such that subsequent low-frequency stimulation evoked biphasic excitatory/inhibitory responses in a CA3 pyramidal cell, an effect lasting for minutes. Analysis of the unitary connections in the circuit revealed that granule cell bursting caused powerful activation of an inhibitory network, thereby transiently suppressing excitatory input to CA3 pyramidal cells. This phenomenon reflects the high incidence of spike-to-spike transmission at granule cell to interneuron synapses, the numerically much greater targeting by mossy fibers of inhibitory interneurons versus principal cells, and the extensively divergent output of interneurons targeting CA3 pyramidal cells. Thus, mossy-fiber input to CA3 pyramidal cells appears to function in three distinct modes: a resting mode, in which synaptic transmission is ineffectual because of high failure rates; a bursting mode, in which excitation predominates; and a postbursting mode, in which inhibitory input to the CA3 pyramidal cells is greatly enhanced. A mechanism allowing the transient recruitment of inhibitory input may be important for controlling network activity in the highly interconnected CA3 pyramidal cell region.

hippocampal mossy fibers | slice cultures | synaptic plasticity | paired recording | feed-forward inhibition

The hippocampal mossy-fiber system is considered to be a major source of excitatory input to the CA3 area of the hippocampus. Histological examination has shown, however, that mossy fibers innervate many more inhibitory interneurons than CA3 pyramidal cells (1), leading to pronounced feed-forward inhibition (2–5). We have recently demonstrated that mossy-fiber feed-forward inhibition is imposed on the network at the level of the unitary circuit among a granule cell, its targeted CA3 pyramidal cells, and the intercalated inhibitory interneurons in the stratum lucidum (6). In the present work we examine the effects of short-term plasticity on the net output of mossy-fiber circuits. Short-term and long-term plasticity have been well characterized at the excitatory synapses from mossy fibers to CA3 pyramidal cells and at the synapses to the stratum lucidum interneurons mediating feed-forward inhibition (5, 7–12). However, because granule cells exhibit divergent connectivity to principal cells and inhibitory interneurons (13), it is of interest to examine the potential functional consequences of differential changes in gain at excitatory versus inhibitory mossy-fiber synapses, which may confer unforeseen properties on the network.

In prior investigations of the mossy-fiber pathway, extracellular stimulation protocols were used that activate numerous neighboring granule cells simultaneously. Computational analysis, however, indicates that this experimental condition is unphysiological because a CA3 pyramidal cell does not receive excitatory input from >1 of the ≈ 50 connected granule cells at any given time (14). Minimal stimulation protocols partially circumvent these problems, but this method suffers from the drawback that the number of stimulated mossy fibers cannot be determined unequivocally, and potentially important subsets of physiological inputs with higher thresholds may be excluded. Furthermore, to facilitate the induction of plasticity, responses were often examined under conditions of inhibitory blockade, which will obscure the role of feed-forward inhibition. To analyze synaptic mechanisms precisely, we have therefore recorded from functionally coupled pairs of neurons, which ensures that only one mossy fiber is stimulated, thereby avoiding potential complications in the interpretation of data arising from synaptic cooperativity and pooling of neurotransmitter.

Granule cells *in vivo* typically fire at frequencies <0.5 Hz except when the animal enters the cell's place field, in which case intermittent bursts at ≈ 40 Hz occur (15). An important goal of this work was therefore to examine how, in the absence of pharmacological intervention, short bursts of action potentials (APs) evoked in a single granule cell modulate the output of a unitary mossy-fiber circuit as determined by recording from a targeted CA3 pyramidal cell. Previous studies have shown high frequency firing to be necessary for mossy-fiber transmission (6, 16, 17). Here, we focused on the period immediately after brief bursting in a single granule cell and observed a transient but significant facilitation of network inhibition.

Results

We characterized short-term facilitation of synaptic transmission in the hippocampal mossy-fiber unitary circuit, which we define as the excitatory connection between a granule cell and a CA3 pyramidal cell in association with the inhibitory feed-forward interneurons targeting that same CA3 pyramidal cell. Because it is presently not possible to obtain patch-clamp recordings from synaptically coupled pairs of granule cells and CA3 pyramidal cells *in vivo* or in acute slices, we used entorhinal–hippocampal slice cultures. Although some modification of circuits occurs in slice cultures primarily in the CA1 area, the connectivity of granule cells and the number of mossy-fiber contacts in the CA3 area have previously been shown to match closely with the morphological characteristics observed *in vivo* (6, 18).

To find synaptically coupled cell pairs, single APs were induced at 1 Hz because lower frequencies are associated with a high failure rate (6). Evoked unitary responses in CA3 pyramidal cells consist of a brief inward current followed by a prolonged outward current (Fig. 1 *A* and *B*). On the basis of

Author contributions: M.M., B.H.G., and U.G. designed research; M.M. performed research; M.M. and U.G. analyzed data; and M.M., B.H.G., and U.G. wrote the paper.

The authors declare no conflict of interest.

Abbreviations: AMPA, α-amino-3-hydroxy-5-methyl-4-isoxazolepropionic acid; AP, action potential; LTP, long-term potentiation; NBQX, 2,3-dihydroxy-6-nitro-7-sulfamoylbenzo[*f*]-quinoxaline.

*To whom correspondence should be addressed. E-mail: mori@hifo.unizh.ch.

This article contains supporting information online at www.pnas.org/cgi/content/full/0702164104/DC1.

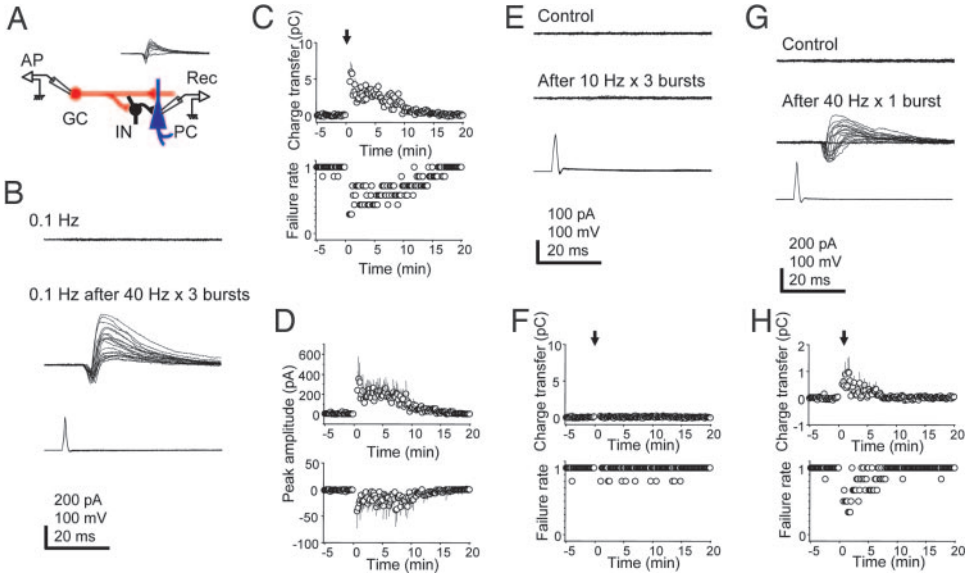

Fig. 1. Granule cell (GC) bursting results in short-term facilitation of synaptic transmission. (*A*) Experimental configuration for recording from a GC–pyramidal cell (PC) pair in a mossy-fiber unitary circuit. (*Inset*) Biphasic mossy-fiber responses evoked in a targeted CA3 PC (−70 mV) by single APs in a GC at 1 Hz. (*B*) Single APs induced at 0.1 Hz in a GC (*Bottom*) fail to evoke responses in a CA3 PC (*Top*). After 40-Hz bursts of APs in the GC (three trains of 2.5-s duration every 10 s), single APs at 0.1 Hz reliably evoke unitary responses in the PC for minutes (*Middle*). (*C*) (*Upper*) Plot of the evoked responses (calculated charge transfer) over time ($n = 7$). The arrow indicates the time when GC bursting was induced. (*Bottom*) Plot of pooled synaptic failures over time ($n = 7$). The seemingly quantal jumps in the failures plot reflect the pooled all-or-none responses from the individual cells. (*D*) Peak amplitude of currents over time is shown for the IPSCs and the EPSCs, respectively. (*E*) Single APs induced at 0.1 Hz in a GC fail to evoke responses in a synaptically connected CA3 PC, both before (*Top*) and after (*Middle*) 10-Hz bursts of APs in the GC (three trains, 10-s duration). (*F*) Plots of charge transfer and failure rates over time. (*G*) Single APs induced at 0.1 Hz in a GC that fail to evoke responses in a synaptically connected CA3 PC successfully evoke responses after a single 40-Hz burst of 2.5 s in the GC. (*H*) Plots of charge transfer and failure rates over time. [Scale bars: vertical, 200 pA (PC, *B* and *G*), 100 pA (PC, *E*), 100 mV (GC); horizontal, 20 ms.]

previously described criteria (6), it is clear that the inward current represents a monosynaptic excitatory connection, whereas the outward current results from disynaptic feed-forward inhibition mediated by stratum lucidum interneurons. Thus, addition of the α-amino-3-hydroxy-5-methyl-4-isoxazolepropionic acid (AMPA)/kainate receptor antagonist 2,3-dihydroxy-6-nitro-7-sulfamoylbenzo[*f*]quinoxaline (NBQX; 10 μM) abolished both inward and outward currents ($n = 4$; data not shown and ref. 6).

Once paired recording was established, the frequency of AP induction in the granule cell was reduced to 0.1 Hz, corresponding to *in vivo* resting rates (15), which resulted in a synaptic failure rate of 0.98 ± 0.01 ($n = 7$) (Fig. 1*C*). If the granule cell was induced to fire three 2.5-s bursts of APs at 40 Hz at 10-s intervals, single APs at 0.1 Hz now reliably evoked responses for 14.2 min (Fig. 1 *B–D*). Quantification of the biphasic responses yielded a net peak charge transfer of 5.93 ± 1.39 pC ($n = 7$). Especially striking was the marked decrease in synaptic failures (Fig. 1*C*). In general, failures covaried [supporting information (SI) Fig. 4], but in 39 of 840 responses (4.6%), failures were observed in the excitatory or the inhibitory component ($n = 7$). Moreover, both inward as well as the outward currents were facilitated (Fig. 1*D*).

If a granule cell was stimulated to fire the same number of APs but distributed over three trains at 10 Hz, frequency facilitation subsided in <10 s, and thereafter unitary responses were rarely evoked (failure rate: before bursts, 0.99 ± 0.01; after bursts, 0.96 ± 0.02; $P = 0.24$; Fig. 1 *E* and *F*). However, a single 2.5-s burst at 40 Hz in the granule cell was sufficient to facilitate synaptic transmission transiently (0.97 ± 0.52 pC; $n = 6$). (Fig. 1 *G* and *H*). When an intermediate frequency of 20 Hz was used, the peak charge transfer after three trains was 1.28 ± 0.22 pC ($n = 3$; data not shown).

To determine which synapses of the mossy-fiber circuit are involved in short-term facilitation of transmission, we examined separately the effect of burst firing at each synapse in the circuit. We first studied the excitatory monosynaptic connection between granule cells and CA3 pyramidal cells under conditions where inhibitory postsynaptic currents (IPSCs) were suppressed (see *Experimental Procedures*). The kinetics for monosynaptic excitatory postsynaptic currents (EPSCs) (Fig. 2*A* and ref. 6) were: peak conductance, 2.3 ± 0.3 nS; 20–80% rise time, 1.6 ± 0.2 ms; and decay time constant, 12.8 ± 1.1 ms ($n = 7$). Transmission at this synapse was not effective when the granule cell was made to fire at a rate of 0.1 Hz (Fig. 2*A*). After the granule cell burst protocol (3 × 40 Hz for 2.5 s), single APs induced at 0.1 Hz in the granule cell evoked EPSCs faithfully, and unitary charge transfer increased transiently (peak, −1.73 ± 0.61 pC; $n = 6$) and then gradually decreased to 0 within 15 min (Fig. 2*A*). Similar properties were observed at the mossy-fiber synapse onto stratum lucidum inhibitory interneurons in which transmission was also ineffective at low frequency (0.1 Hz). Again, the reliability of unitary synaptic transmission was increased after three 40-Hz bursts of the granule cell, and the unitary charge transfer was increased (peak, −0.80 ± 0.28 pC; $n = 10$; Fig. 2*B*). In contrast to the synapses from mossy fibers to CA3 pyramidal cells or to interneurons, the synapse from stratum lucidum interneurons to CA3 pyramidal cells effectively transmitted unitary GABAergic outward currents at a frequency of 0.1 Hz (Fig. 2*C*). Moreover, neither failure rate (before bursts, 0.056 ± 0.015; after bursts, 0.039 ± 0.013; $P = 0.40$) nor charge transfer (before bursts, 0.36 ± 0.01 pC; after bursts, 0.35 ± 0.01 pC; $P = 0.53$) was significantly changed after interneuron bursting (3 × 40 Hz for 2.5 s). The kinetics for the IPSCs were: peak conductance, 1.9 ± 0.4 nS; 20–80% rise time, 2.2 ± 0.5 ms; and decay time constant, 13.7 ± 3.4 ms ($n = 5$). Although IPSCs were depressed after bursting (6), this effect recovered within

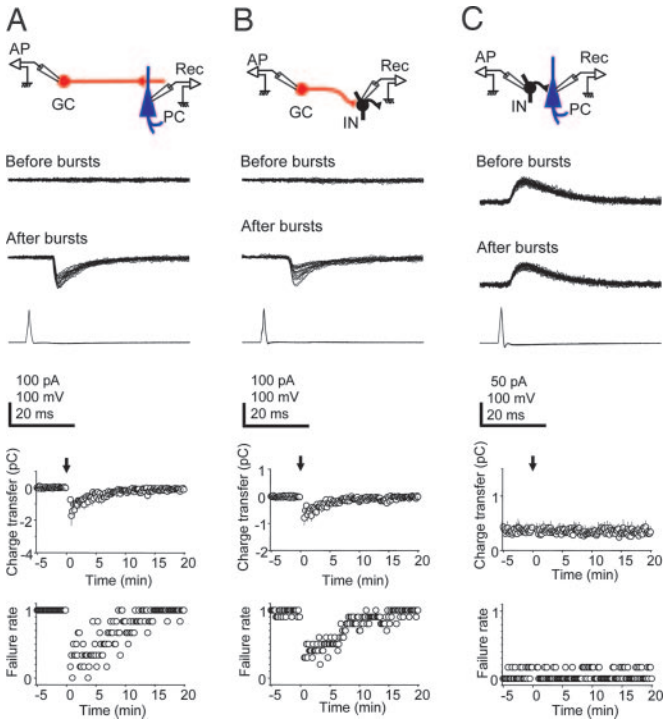

Fig. 2. Characterization of the synapses involved in postburst facilitation. Postburst enhancement of monosynaptic responses occurs at mossy-fiber synapses onto CA3 pyramidal cells (PC) (*A*) and interneurons (INs) (*B*). Single APs induced at 0.1 Hz in a granule cell (GC) (*Bottom traces*) fail to evoke responses in the synaptically coupled PC or IN (*Top trace*), but after GC bursting (3 × 40 Hz) single GC APs at 0.1 Hz evoke monosynaptic excitatory currents in target cells (*Middle traces*; superimposed traces during first 3 min after bursting). (*A*) IPSCs in PCs were suppressed. (*Lower*) Plots of the changes over time in synaptic charge transfer, and synaptic failure rate ($n = 6$ for PCs, $n = 10$ for INs), with arrows indicating time of GC bursting. (*C*) In contrast, the IN to CA3 PC synapse is not sensitive to IN bursting. Single APs even at 0.1 Hz in an IN reliably evoke GABAergic unitary responses in a PC (*Top trace*). IN bursting at 40 Hz does not change transmission (*Middle trace*). (*Lower*) Plots of charge transfer and failure rate over time ($n = 6$). [Scale bars: vertical, 100 pA (PC and IN), 100 mV (GC); horizontal, 20 ms.]

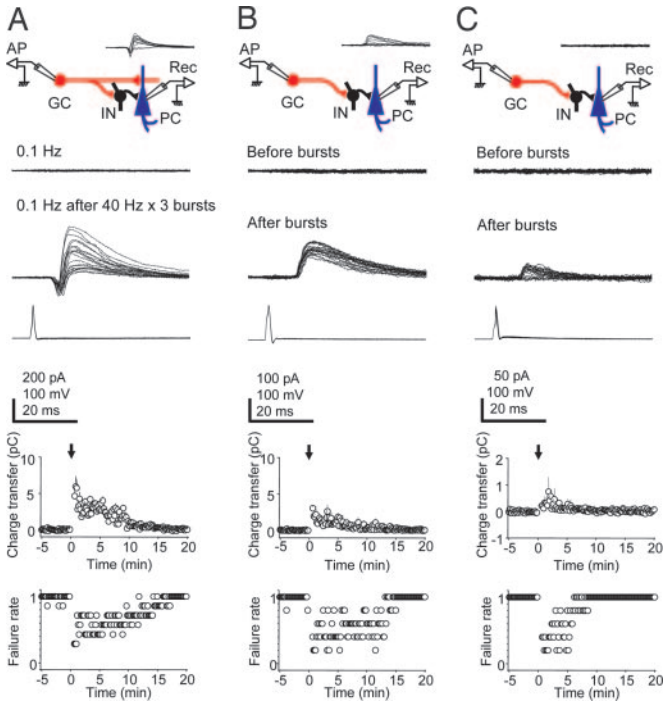

Fig. 3. Comparison of postburst feed-forward inhibition in CA3 pyramidal cells with or without a monosynaptic excitatory input. (*A*) The same traces as in Fig. 1*B* showing unitary biphasic responses in a pyramidal cell after granule cell bursting. (*B*) A CA3 pyramidal cell that is disynaptically driven by a granule cell firing at 1 Hz (*Inset*) by an inhibitory neuron but without a monosynaptic excitatory input. At 0.1 Hz (*Top trace*), single APs in the granule cell did not evoke IPSCs in the CA3 pyramidal cell (−70 mV). Following the 3 × 40 Hz bursting protocol, granule cell APs at 0.1 Hz reliably evoke IPSCs (*Middle trace*), which were, however, of lesser amplitude than in the pairs depicted in *A*. (*C*) (*Upper*) Postburst appearance of disynaptic inhibitory responses in previously silent granule cell–pyramidal cell pairs (*Inset*). Single APs in a granule cell at 0.1 Hz (*Bottom trace*) fail to evoke synaptic responses in a pyramidal cell (*Top trace*), but after granule cell bursting (3 × 40 Hz) single granule cell APs at 0.1 Hz transiently evoked disynaptic inhibitory responses in the pyramidal cell (*Middle trace*), albeit of low amplitude. (*Lower*) Plots of synaptic charge transfer and failure rate over time ($n = 5$). [Scale bars: vertical, 100 pA (IN, *A*; PC, *C*), 50 pA (PC, *B*), 100 mV (GC, *A* and *C*; IN, *B*); horizontal, 20 ms.]

seconds and was therefore not apparent at a discharge frequency of 0.1 Hz.

The prominent facilitation of outward current observed after granule cell bursting (Fig. 1*B*) implies that the mossy-fiber synapse mediates suprathreshold or spike-to-spike transmission at interneurons targeting the CA3 pyramidal cell, as reported previously (6, 17, 19, 20). To test whether this property is modified by granule cell bursting, the reliability of spike-to-spike transmission was monitored in granule cell–interneuron pairs in which synaptically evoked APs were recorded from stratum lucidum interneurons in the loose cell-attached mode. Indeed, mossy-fiber APs induced at 0.1 Hz consistently evoked APs in the interneurons for 9.2 min after bursting of granule cells (3 × 40 Hz; $n = 7$; SI Fig. 5).

Feed-forward inhibition can play a role in limiting the time window for synaptic integration (21), or it might serve to enhance signaling to a target cell through a mechanism involving lateral inhibition (5). If mossy-fiber activation would result in pronounced surround inhibition, disynaptic lateral inhibition in the neighboring cells should be more pronounced than feed-forward inhibition onto the monosynaptically targeted CA3 pyramidal cell. To examine this issue, we compared the inhibitory component of responses in CA3 pyramidal cells with a monosynaptic mossy-fiber connection (Fig. 3*A*) versus responses in neighboring cells exhibiting only a disynaptic inhibitory component. In five cases, we found granule cell–CA3 pyramidal cell pairs in which a presynaptic AP evoked only an inhibitory postsynaptic response, indicating that the two cells were coupled by intercalated inhibitory interneurons and not by a monosynaptic excitatory connection (Fig. 3*B*). These responses were blocked completely by 10 μM NBQX, consistent with disynaptic feed-forward inhibition (data not shown). Lowering the frequency of granule cell APs from 1 Hz to 0.1 Hz resulted in the failure of evoked responses in the CA3 pyramidal cell (Fig. 3*B*). After granule cell bursting, the success rate for evoking disynaptic inhibitory responses was increased. Furthermore, the outward charge transfer attained a peak of 3.05 ± 0.17 pC ($n = 5$; Fig. 3*B*). Thus, synaptic charge transfer in cell pairs not monosynaptically coupled was somewhat lower than in monosynaptically coupled pairs (5.93 ± 1.39 pC, $n = 7$, $P = 0.12$; Fig. 3*A*), suggesting that any signal enhancement occurring at a targeted CA3 cell by mossy-fiber-mediated lateral inhibition will be offset by the powerful feed-forward inhibition. It should be noted that in the monosynaptically coupled pairs, the value of 5.93 pC is an underestimation of inhibition because of the temporal overlap with the preceding excitatory component (−1.73 ± 0.61 pC, $n = 6$).

Stratum lucidum interneurons exhibit extensively ramifying axonal arbors targeting CA3 pyramidal cells (22–25). On the

basis of this axonal divergence, we predicted that after granule cell bursting one should recruit disynaptic feed-forward inhibitory responses in a proportion of previously silent granule cell–CA3 pyramidal cell pairs. To test this hypothesis, we recorded randomly from granule cell–CA3 pyramidal cell pairs. Consistent with an estimated probability of connectivity of 0.0046% (26), synaptic transmission was not observed in the 14 pairs tested. However, after granule cell bursting (3×40 Hz for 2.5 s), disynaptic inhibition in the absence of synaptic excitation was observed in 6 of the 14 cell pairs (43%; Fig. 3*C*). After granule cell bursting, outward charge transfer reached a peak of 0.75 ± 0.54 pC ($P = 0.01$), and disynaptic inhibitory responses were observed for 8.5 min ($n = 5$; Fig. 3*C*). In this case, charge transfer was lower (Fig. 3*C*) than in those pairs exhibiting a disynaptic inhibitory response from the outset (Fig. 3*B*), suggesting that even fewer interneurons were targeting the CA3 pyramidal cell.

Discussion

Our results demonstrate that brief bursting in just one granule cell subsequently induces a profound increase in network inhibition that can last for minutes, even though the immediately preceding mossy-fiber excitatory response is also facilitated (5, 8, 11). This finding can be explained by the ≈10-fold greater targeting by mossy fibers of inhibitory interneurons than CA3 pyramidal cells (1) and by the spike-to-spike transmission observed even at low discharge frequencies between granule cells and interneurons (6, 17, 19, 20). A transient increase in disynaptic inhibition after granule cell bursting appears also to occur in behaving animals as evidenced by the phenomenon of dentate spikes, which are observed during immobility, consummatory behavior, and slow-wave sleep (27, 28). This hippocampal response is characterized by synchronous activity within the dentate region, leading to a marked suppression of activity in CA1 and CA3 pyramidal cells.

A second finding from our study was that the interneurons receiving input from a given granule cell focus their output strongly onto the CA3 pyramidal cells innervated by that same granule cell, with inhibitory drive falling off progressively for CA3 pyramidal cells synaptically distant from the targeted cell (Fig. 3). Feed-forward inhibition to those CA3 pyramidal cells that were targeted by the bursting granule cell thus is greater than lateral inhibition onto neighboring cells. This observation suggests that lateral inhibition in the mossy-fiber pathway, which would emphasize monosynaptic excitation by selectively depressing activity in surrounding cells, is offset by the powerful feed-forward inhibition onto the target cell.

Previously we demonstrated that with increasing firing rates of a single granule cell, intrinsic synaptic mechanisms induce an immediate switching from predominantly inhibition to predominantly excitation of targeted CA3 pyramidal cells (6). Here, we find that bursting by a granule cell, which briefly excites CA3 pyramidal cells (6, 16, 17), subsequently triggers a form of short-term plasticity resulting in enhanced inhibitory drive, such that activity in a previously bursting granule cell will depress CA3 pyramidal cells within the sphere of the facilitated network of interneurons. Taken together, these findings suggest that mossy-fiber input to the CA3 pyramidal cells functions in three distinct modes: (*i*) a resting mode, in which synaptic transmission is ineffectual because of high failure rates; (*ii*) a bursting mode, corresponding, e.g., to the presence of an animal within the cell's place field, in which excitation is successfully transmitted to targeted pyramidal cells; and (*iii*) a postbursting mode immediately thereafter, in which inhibition to CA3 pyramidal cells is greatly enhanced.

In our experiments we observed increased inhibitory drive that lasted up to 15 min after three trains of 100 APs at 40 Hz (Fig. 1*C*). This type of stimulation protocol consisting of repetitive tetanic trains is commonly used to induce synaptic plasticity even though sustained place field activity of granule cells *in vivo* is of much shorter duration (15). It is nonetheless useful to drive a system toward its maximum to facilitate analysis of synaptic mechanisms. However, we also examined the effects of a single 40-Hz train of 2.5-s duration containing 100 APs, which is comparable in terms of mean frequency to the physiological activity recorded from a granule cell when an animal is moving through the cell's place field [e.g., 46 spikes during 1.8 s (figure 5*A* in ref. 17)]. After a single 40-Hz burst, peak inhibition was observed for ≈2 min and then gradually diminished to control levels within 7 min (Fig. 1 *G* and *H*).

Measurement of charge transfer at the synapses in the mossy-fiber circuit permits us to estimate the number of inhibitory interneurons that can be recruited after granule cell bursting. The unitary outward charge transfer at interneuron–pyramidal cell synapses, which does not vary after interneuron bursting, is 0.35 pC (Fig. 2*C*). The peak inhibitory charge transfer after granule cell bursting was 5.93 pC outward for disynaptic feed-forward inhibition associated with monosynaptic excitatory transmission (Fig. 3*A*), 3.05 pC for disynaptic inhibition without a monosynaptic excitatory connection (Fig. 3*B*), and 0.75 pC when disynaptic inhibition was revealed only after granule cell bursting (Fig. 3*C*). These numbers indicate that the CA3 pyramidal cell received input from at least 17, 9, and 3 interneurons, respectively, in response to a single AP in the granule cell. Feed-forward inhibition will occur in only ≈12 monosynaptically connected CA3 pyramidal cells (1, 6) (SI Fig. 6) of an estimated total of 5,000 CA3 pyramidal cells in a slice culture, or 0.24%, whereas 43% of CA3 pyramidal cells (Fig. 3*C*) received lateral inhibition. However, even though lateral inhibition is more prevalent spatially in the mossy-fiber circuit, feed-forward inhibition is greater in magnitude.

The stratum lucidum interneurons from which we recorded were generally aspiny with a bipolar dendritic arborization extending into the stratum radiatum and stratum oriens (6). These interneurons correspond closely to the previously characterized mossy-fiber-associated interneurons in stratum lucidum, whose massively branching axons innervate several hundred CA3 pyramidal cells (24), explaining our finding that disynaptic inhibition was observed even in granule cell–CA3 pyramidal cell pairs lacking a monosynaptic connection. Mossy-fiber arborization in slice cultures is similar to that reported *in vivo* with comparable numbers of excitatory large mossy-fiber boutons, filopodial extensions, and *en passant* varicosities (6, 18), undergoing similar activity-dependent changes in connectivity (29).

Postburst recruitment of inhibitory interneurons may be of importance in a variety of physiological processes. A major function of feed-forward inhibition is to impose a time window for coincidence detection in postsynaptic cells (30). However, the comparatively long duration of enhanced net inhibitory transmission observed after a granule cell burst implies additional roles, for example, in the heterosynaptic plasticity between CA3 pyramidal cells (31). If mossy-fiber input is considered to provide the depolarizing signal that permits NMDA receptor-dependent associative long-term potentiation (LTP) within the CA3 recurrent network (31–35), a mechanism to suppress CA3 input transiently is necessary to stabilize LTP. Otherwise, the initial expression of LTP between CA3 pyramidal cells, which depends on the insertion of new AMPA receptors into the synapse, would be disturbed. This process of LTP-dependent AMPA receptor trafficking takes between 20 and 40 s (36–38). Accordingly, continued stimulation after LTP induction prevents synaptic potentiation, as shown *in vitro* (39) and *in vivo* (40). We thus propose that transient curtailment of excitatory input to a CA3 pyramidal cell, which was depolarized by a mossy fiber to allow LTP at synapses with its neighboring CA3 cells, may represent

a mechanism to protect synapses undergoing potentiation from disruptive input.

Periods of increased inhibitory drive to the CA3 network may also be involved in modulating interactions between the entorhinal cortex and each of the hippocampal subfields. Recent studies have established that the entorhinal cortex generates the primary representation of space (41), whereas the CA1 and the CA3 regions integrate entorhinal input with distinct contextual features (42, 43). Thus, for certain behavioral and memory functions, the entorhinal cortex communicates selectively with the CA1 area to the exclusion of CA3 (33, 44–46). In such cases, a temporary disconnection of the sequential trisynaptic circuit from entorhinal cortex to granule cells, CA3, and CA1 pyramidal cells would be required. Extensive postburst enhancement of feed-forward inhibition to the CA3 network, possibly through the generation of dentate spikes, may serve as the mechanism to interrupt CA3 to CA1 transmission during periods of entorhinal excitation of the CA1 area.

Experimental Procedures

Slice Culture Preparation. All experiments were carried out on slice cultures prepared from 6-day-old Wistar rat pups killed by decapitation following a protocol approved by the Veterinary Department of the Canton of Zurich. Hippocampal slices including the entorhinal cortex were sectioned at 400 μm, attached to glass coverslips with clotted chicken plasma, placed in sealed test tubes with serum-containing medium, and kept in a roller-drum incubator at 36°C for 21–28 days (47).

Electrophysiology. Cultures were transferred to a recording chamber mounted on an upright microscope (Axioskop FS1; Zeiss, Jena, Germany) and superfused with an external solution (pH 7.4) containing 148.8 mM Na^+, 2.7 mM K^+, 149.2 mM Cl^-, 2.8 mM Ca^{2+}, 2.0 mM Mg^{2+}, 11.6 mM HCO_3^-, 0.4 mM $H_2PO_4^-$, 5.6 mM D-glucose, and 10 mg/liter phenol red (pH 7.4). All experiments were performed at 34°C. Recordings were obtained from pyramidal cells in the area CA3a and b, dentate granule cells, and CA3 stratum lucidum interneurons with patch pipettes (2–5 MΩ) by using an Axopatch 200B amplifier (Axon Instruments, Foster City, CA).

For current-clamp recording in granule cells and all voltage-clamp recordings except those in Figs. 2 and 3*A*, pipettes were filled with 135 mM potassium gluconate/5 mM KCl/10 mM Hepes/1 mM EGTA/2 mM Mg-ATP/5 mM creatine phosphate (CrP)/0.4 mM GTP/0.07 mM $CaCl_2$, pH 7.2. For voltage-clamp recordings shown in Figs. 2 and 3*A*, patch pipettes were filled with 121.6 mM CsF/8.4 mM CsCl/10 mM Hepes/10 mM EGTA/1 mM picrotoxin/2 mM Mg-ATP/5 mM CrP/0.4 mM GTP, pH 7.2. For loose cell-attached patch recordings, pipettes were filled with external solution. In some experiments, IPSCs were suppressed by an intracellular solution with fluoride as the major anion and to which the $GABA_A$ receptor antagonist picrotoxin was added, and by adjusting the equilibrium potential for chloride to correspond to the holding potential of −70 mV. Membrane potentials were corrected for junction potentials. Presynaptic APs were evoked by injecting depolarizing current (1 ms, 1.5–2 nA) at 0.1 Hz unless otherwise mentioned. To facilitate the search for a synaptically coupled cell pair, we first obtained a stable recording from a postsynaptic CA3 pyramidal cell and then systematically scanned the dentate gyrus with a potassium puff electrode (140 mM K^+) to induce localized activation of a small number of granule cells. This method of identifying areas with presynaptically connected cells (potassium puff search) yielded a success rate of ≈10%. A functional connection was confirmed initially by evoking synaptic responses at 1 Hz in the postsynaptic cell held at −70 mV. Series resistance (5–15 MΩ) was monitored regularly, and cells were excluded if a change of >20% occurred.

Drugs and Chemicals. NBQX was purchased from Tocris Cookson (Bristol, U.K.). ATP, CrP, EGTA, GTP, and picrotoxin were from Sigma (St. Louis, MO)/Fluka (Buchs, Switzerland).

Data Acquisition and Analysis. Signals were filtered at 5 or 10 kHz, digitally recorded with CLAMPEX 7 software (Axon Instruments), and stored on hard disk for later analysis. Amplitude, latency, and kinetics were determined by using a standard protocol (48). Charge transfer was calculated by integrating postsynaptic currents for 45 ms after each AP. Net charge transfer for EPSC/IPSC sequences was measured by subtracting the charge produced by inward currents from that carried by outward currents. Failure rate was plotted as the ratio of the number of the neurons without a unitary response to the total number of neurons studied. The duration of facilitated transmission was taken as the time until the failure rate of the cell pair again exceeded 0.8. Numerical data are expressed as means ± SEM. Student's *t* test was used to compare values when appropriate.

We thank S. Giger, H. Kasper, L. Rietschin, and R. Schöb for excellent technical assistance and Dr. M. H. Abegg for discussion and the camera lucida figure. This work was supported by the Swiss National Science Foundation (U.G.), the National Center of Competence in Research on Neural Plasticity and Repair (U.G.), and the Sumitomo Foundation (M.M.).

1. Acsády L, Kamondi A, Sík A, Freund T, Buzsáki G (1998) *J Neurosci* 18:3386–3403.
2. Brown TH, Johnston D (1983) *J Neurophysiol* 50:487–507.
3. Frotscher M (1989) *Exp Brain Res* 75:441–445.
4. Frotscher M (1985) *J Neurocytol* 14:245–259.
5. Lawrence JJ, McBain CJ (2003) *Trends Neurosci* 26:631–640.
6. Mori M, Abegg MH, Gähwiler BH, Gerber U (2004) *Nature* 431:453–456.
7. Zalutsky RA, Nicoll RA (1990) *Science* 248:1619–1624.
8. Salin PA, Scanziani M, Malenka RC, Nicoll RA (1996) *Proc Natl Acad Sci USA* 93:13304–13309.
9. Yeckel MF, Kapur A, Johnston D (1999) *Nat Neurosci* 2:625–633.
10. Henze DA, Urban NN, Barrionuevo G (2000) *Neuroscience* 98:407–427.
11. Nicoll RA, Schmitz D (2005) *Nat Rev Neurosci* 6:863–876.
12. Pelkey KA, Topolnik L, Lacaille JC, McBain CJ (2006) *Neuron* 52:497–510.
13. Tóth K, McBain CJ (2000) *J Physiol (London)* 525:41–51.
14. Lisman JE (1999) *Neuron* 22:233–242.
15. Jung MW, McNaughton BL (1993) *Hippocampus* 3:165–182.
16. Geiger JR, Jonas P (2000) *Neuron* 28:927–939.
17. Henze DA, Wittner L, Buzsáki G (2002) *Nat Neurosci* 5:790–795.
18. De Paola V, Arber S, Caroni P (2003) *Nat Neurosci* 6:491–500.
19. Lawrence JJ, Grinspan ZM, McBain CJ (2004) *J Physiol (London)* 554:175–193.
20. Miles R (1990) *J Physiol (London)* 431:659–676.
21. Mittmann W, Chadderton P, Hausser M (2004) *Curr Biol* 14:R837–R839.
22. Gulyás AI, Miettinen R, Jacobowitz DM, Freund TF (1992) *Neuroscience* 48:1–27.
23. Spruston N, Lubke J, Frotscher M (1997) *J Comp Neurol* 385:427–440.
24. Vida I, Frotscher M (2000) *Proc Natl Acad Sci USA* 97:1275–1280.
25. Aaron GB, Wilcox KS, Dichter MA (2003) *Neuroscience* 117:169–181.
26. Amaral DG, Ishizuka N, Claiborne B (1990) *Prog Brain Res* 83:1–11.
27. Bragin A, Jando G, Nadasdy Z, van Landeghem M, Buzsáki G (1995) *J Neurophysiol* 73:1691–1705.
28. Penttonen M, Kamondi A, Sík A, Acsády L, Buzsáki G (1997) *Hippocampus* 7:437–450.
29. Galimberti I, Gogolla N, Alberi S, Santos AF, Muller D, Caroni P (2006) *Neuron* 50:749–763.
30. Pouille F, Scanziani M (2001) *Science* 293:1159–1163.
31. Kobayashi K, Poo MM (2004) *Neuron* 41:445–454.
32. McNaughton B, Morris RGM (1987) *Trends Neurosci* 10:408–415.
33. Buzsáki G (1989) *Neuroscience* 31:551–570.
34. Chattarji S, Stanton PK, Sejnowski TJ (1989) *Brain Res* 495:145–150.
35. Nakazawa K, Quirk MC, Chitwood RA, Watanabe M, Yeckel MF, Sun LD, Kato A, Carr CA, Johnston D, Wilson MA, Tonegawa S (2002) *Science* 297:211–218.

36. Gustafsson B, Asztely F, Hanse E, Wigström H (1989) *Eur J Neurosci* 1:382–394.
37. Petersen CC, Malenka RC, Nicoll RA, Hopfield JJ (1998) *Proc Natl Acad Sci USA* 95:4732–4737.
38. Bagal AA, Kao JP, Tang CM, Thompson SM (2005) *Proc Natl Acad Sci USA* 102:14434–14439.
39. Abraham WC, Huggett A (1997) *Hippocampus* 7:137–145.
40. Stäubli U, Scafidi J (1999) *J Neurosci* 19:8712–8719.
41. Leutgeb S, Leutgeb JK, Moser EI, Moser MB (2005) *Curr Opin Neurobiol* 15:738–746.
42. Leutgeb S, Leutgeb JK, Treves A, Moser MB, Moser EI (2004) *Science* 305:1295–1298.
43. Leutgeb S, Leutgeb JK, Moser EI, Moser MB (2006) *Hippocampus* 16:765–774.
44. Frank LM, Brown EN, Wilson MA (2000) *Neuron* 27:169–178.
45. Brun VH, Otnass MK, Molden S, Steffenach HA, Witter MP, Moser MB, Moser EI (2002) *Science* 296:2243–2246.
46. Remondes M, Schuman EM (2004) *Nature* 431:699–703.
47. Gähwiler BH (1988) *Trends Neurosci* 11:484–489.
48. Feldmeyer D, Egger V Lubke J, Sakmann B (1999) *J Physiol (London)* 521:169–190.